ISSN: 1813-4890

Route distribution and facility layout optimization for Ro-Ro passenger ship during evacuation from main vertical zone

Xiaofan Yuan, Yuqiang Sun, Lu Ding, Jun Jiang and Jinnan Yu

School of navigation and shipping, Shandong Jiaotong University, Weihai 264200, China.

Abstract

Ro-Ro (roll-on roll-off) passenger ships are divided into several main vertical zones (MVZs) by fireproof bulkheads to limit the fire spread. Considering differences in personnel conflict risk across various passage segments, this study proposes an evacuation facility layout optimization method during evacuation from main vertical zone based on a route distribution model and K-means clustering. Firstly, a topological network for a deck with a single MVZ is constructed. Secondly, considering the probability of choosing each exit, evacuation equivalent unit conflict values are obtained for different passage segments. Thirdly, the main areas for arranging evacuation signs and markings are determined by conflict risk on different passage segments. The results show that the highest value of conflict equivalent occurs at the intersection. This study determines the distance ratio of each channel section based on the position of MVZ in the longitudinal profile of the ship, which provides decision support for evacuation layout optimization of facilities and surveillance cameras.

Keywords

Ro-Ro passenger ship, Personnel conflict, Path allocation, Clustering, Main vertical zone.

1. Introduction

Ro-Ro passenger ships feature a unique multi-deck structure, typically consisting of horizontal decks and MVZs. An MVZ is a vertical area divided by the ship's fire-resistant structure. In the event of a fire, if it is contained within a manageable scope inside an MVZ, personnel are required to evacuate from the affected zone to safe areas under the guidance of signs, markings and crew members. A critical challenge is how to efficiently organize the evacuation of all personnel within a single MVZ and on a single deck, while allocating suitable exits for each individual. In this context, it is crucial to develop a practical method for allocating evacuation routes during an evacuation process of the Ro-Ro passenger ship.

Fire accidents on Ro-Ro passenger ships have a high potential to cause severe casualties. To limit the spread of fire, the hull is longitudinally divided into several independent main vertical zones by Class A fire-resisting bulkheads. However, this design also necessitates that passengers must evacuate quickly from a fire-affected MVZ, guided by evacuation signs or crew members. Given the complex structure of Ro-Ro passenger ships, rescue and evacuation operations are particularly challenging. Optimizing the layout of evacuation facilities within an MVZ is therefore crucial for improving evacuation efficiency and reducing personnel congestion. Consequently, enhancing the placement of evacuation signs and markings along the routes from the affected MVZ to safe areas is a primary strategy for mitigating fire risks.

During the evacuation process, passengers' behavior in choosing exits is random. The probability of selecting a particular exit is typically determined by a probability distribution model based on a utility function. The utility function is influenced by path length and congestion degrees. It is noteworthy that Ro-Ro passenger ships have sufficient guidance signs and markings to guide personnel toward the nearest evacuation exit. This phenomenon also

has an obvious impact on the utility function. Therefore, evacuation signs and markings have a positive impact on the evacuation process, increasing the probability of passengers choosing relatively closer exits. Besides, the use and selection of various evacuation coefficients have a significant impact on path selection probabilities and the overall evacuation efficiency.

To address the evacuation problem in MVZ of Ro-Ro passenger ships, this study proposes an evacuation layout optimization method based on probability assignment and K-means clustering. The main contributions are summarized as follows.

(1) Considering the shortest path distance from each room to the exit and the total number of rooms, a conflict adjustment coefficient for evacuation equivalent unit conflict value is proposed to correct evacuation difficulty differences for individuals located far from the exit.

(2) To make the results more realistic, this study integrates the impacts of distance congestion and guidance arrows on the utility function of path allocation, and provides the weight coefficient and turning coefficient for path allocation probability.

(3) Evacuation equivalent unit conflict values are clustered by K-means clustering method to analyze the impact of conflict equivalents on evacuation layout from the perspective of evacuation conflicts. This provides decision support for the layout of fire evacuation facilities and surveillance cameras.

The remainder of this study is structured as follows. Section 2 reviews the relevant literature from recent years. Section 3 presents the problem statement, proposes the evacuation equivalent unit conflict value, and provides some basic concepts related to K-means clustering. The solution process for the evacuation problem is also detailed in this section. Section 4 demonstrates the effectiveness of this method by using an empirical example of a Ro-Ro passenger ship, where the evacuation problem for MVZ is solved by the probability model and clustering approach. Finally, Section 5 concludes the main innovations of this study.

2. Literature review

The research on evacuation route planning, probability distribution, and traffic conflict point has received widespread attention.

In terms of evacuation route planning, He et al. proposed a method for multi-hazard accident evacuation route planning in chemical industrial parks based on pre-event and on-site risk perception, utilizing dynamic comprehensive risk analysis as an equivalent distance criterion to enhance the D* algorithm for evacuation route planning [1]. Yang et al. considered the impact of failures in evacuation network component such as turnstiles on route planning, and established a two-stage passenger evacuation route optimization method under flood scenarios in subway stations, aiming to minimize total evacuation time, total risk, and total congestion [2]. Zhang et al. proposed an improved adaptive ant colony algorithm that considers risk, energy consumption, and route length as key factors, while introducing an adaptive pheromone evaporation coefficient to balance convergence and global search capabilities, and visualized the hazard range on a grid map [3]. Rodrigues et al. proposed a multi-objective emergency rescue method by a mixed-integer linear programming model, determining evacuation routes and shelter locations using geographic information systems [4].

In terms of probability assignment, Gu et al. proposed a new multiplicative stochastic regret model with a multiplicative error structure, which addressed the scale invariance problem and better captured travelers' perceptions while maintaining prediction accuracy [5]. Rasmussen et al. introduced a bounded path selection model considering a local detour threshold by using the concept of local detour, to explain route selection behaviors that traditional stochastic user equilibrium models cannot capture [6]. Qin et al. proposed a privacy-preserving traffic assignment framework, introducing differential privacy into the traffic assignment process, injecting noise at the individual travel level, and solving by using chance-constrained

ISSN: 1813-4890

optimization methods, achieving the unification of privacy protection and traffic equilibrium calculation [7].

In terms of traffic conflict point, Islam and Abdel-Aty proposed a novel real-time conflict prediction method that utilizes historical trajectory data of individual vehicles to analyze the potential for conflicts in the near future [8]. Park et al. analyzed the correlation between vehicle conflict indicators and accident frequency, identified high-risk areas within intersections, and provided data support for traffic safety intervention measures [9]. Arun et al. estimated crash frequency based on the severity of conflicts using a multivariate extreme value modeling framework, and analyzed the potential role of multiple conflict indicators in refining conflict-based collision estimation models [10].

3. Material and Method

This section is arranged as follows. Section 3.1 presents a problem description and the overall research framework. Then, a novel evacuation equivalent unit conflict value is proposed to quantify the conflict degree of paths in Section 3.2.

3.1. Problem description

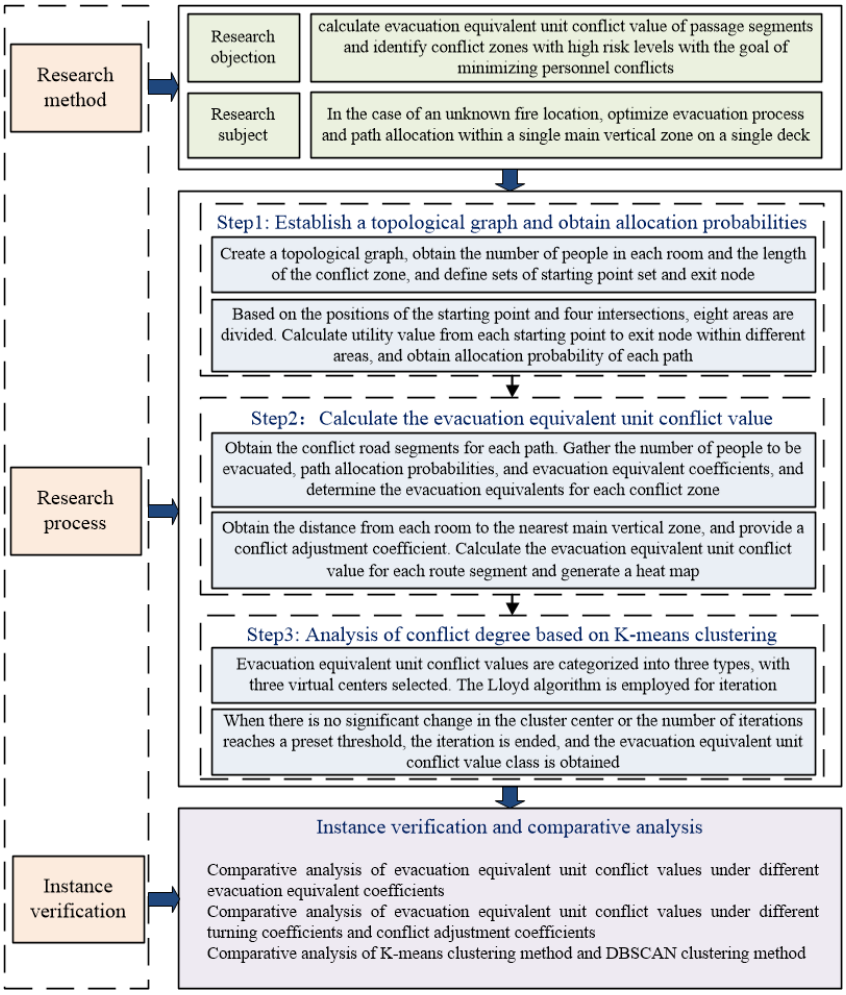

Fig. 1 The overall research framework in this study

The objective of the problem is to minimize the evacuation equivalent unit conflict value and generate a heat map of the evacuation equivalent unit conflict value for each conflict zone, thereby visually identifying the conflict zones where the possibility of personnel falling is high. For convenience, the assumptions are as follows.

(1) Individuals with different starting points have a certain probability of choosing exits.

ISSN: 1813-4890

(2) To maintain objectivity, stair information in the evacuation route image of the Ro-Ro passenger ship is removed.

(3) This study does not consider the situation of people going up and down stairs.

(4) Personnel should prioritize safe evacuation and avoid moving in the opposite direction of the exit.

To solve the problem of evacuation for a single MVZ of Ro-Ro passenger ships, the overall research framework in this study involves three parts. Firstly, a topological network is established and the probability of choosing evacuation routes is obtained. Secondly, the evacuation equivalent unit conflict value of each passage segment is calculated. Thirdly, evacuation equivalent unit conflict value is analysed by K-means clustering method. It is noteworthy that the study adopts a topological network to describe the internal layout of Ro-Ro passenger ships. The ship is modeled as an undirected graph $G=(V,E)$, where $V=S\cup M\cup D$ represents a set of evacuation nodes. $E=\{(i,j)|i\in V,j\in V\}$ represents a set of evacuation routes. $S=\{1,2,\cdots,s\}$, $M=\{1,2,\cdots,m\}$ and $D=\{1,2,\cdots,d\}$ represent sets of starting points, corridor nodes and exit nodes. A conflict zone (i,j) represents a junction where pedestrian flow from different directions converge with a certain probability, indexed by $(i,j)\in E$. Fig. 1 presents the overall research framework of this study. Fig. 2 illustrates the conflict zone schematic. The path allocation from the starting point to the four exits is shown in Fig. 3.

Fig. 2 Schematic diagram of the conflict zone, where the green part is the conflict zone

Fig. 3 Schematic diagram of path allocation for different exits

ISSN: 1813-4890

3.2. Evacuation equivalent unit conflict value

To measure the risk degree in the conflict zone during an evacuation process, this study proposes an evacuation equivalent unit conflict value. During the evacuation process, different evacuation paths assigned to personnel may intersect, thereby forming conflict zones. Based on this, an evacuation equivalent unit conflict value represents the probability of falls on each road segment, which is defined as evacuation equivalent in the conflict zone multiplied by the quotient of the length of the road segment and the length of the conflict zone. In conflict zones, the greater the evacuation equivalent, the longer the road segment, and the shorter the conflict zone length, the greater the evacuation equivalent unit conflict value. Firstly, to obtain the evacuation equivalent unit conflict value, the allocation probability from starting point s to exit node d is defined as

$$p_{sd} = \frac{e^{U_{sd}}}{\sum_{d \in D} e^{U_{sd}}}, \tag{1}$$

where, U_{sd} represents the utility function from starting point s to exit node d. To conform to reality, this study integrates the effects of distance, congestion degree and guidance arrows on evacuation efficiency. Concretely, the utility function from starting point s to exit node d is given as

$$U_{sd} = 1 - \frac{\alpha_d \cdot l_{sd}(\beta \cdot y_{sd} + 1)}{\max\left(\alpha_d \cdot l_{sd}(\beta \cdot y_{sd} + 1)\right)}, \tag{2}$$

where, l_{sd} represents the length of evacuation routes. α_d represents a weight coefficient that assigns weights of 1, 2, 3, and 4 to the four exits in ascending order after sorting them based on l_{sd}. β represents steering coefficient, which is set to 0.5. y_{sd} represents a 0-1 decision variable. If a person turns during the evacuation process, the value is 1. Otherwise, the value is 0. Then, risk equals the probability of occurrence of an accident multiplied by the severity of the consequences [11]. Therefore, evacuation evacuation equivalent of the conflict section (i, j) is given as

$$Q_{sdij} = \gamma \cdot p_{sd} \cdot i_s, \tag{3}$$

where, i_s represents personnel number to be evacuated at the starting point s. γ represents evacuation equivalent coefficient, which is set to 10. It is noteworthy that the evacuation equivalent will be evenly distributed on these two routes if there are two evacuation routes from the starting point to the exit node.

Besides, individuals close to the exit face less evacuation difficulty, while those far from the exit encounter greater evacuation difficulty. Therefore, based on the shortest distance from each starting point to the exit and the total number of starting points, conflict adjustment coefficient of each starting point is given as

$$a_s = \frac{\min\limits_{d \in D}(l_{sd}) \cdot |S|}{\sum\limits_{s \in S} \min\limits_{d \in D}(l_{sd})}, \tag{4}$$

where, $\min\limits_{d \in D}(l_{sd})$ represents the shortest distance from starting point s to exit node d. $|S|$ represents the number of starting points. Finally, according to the conflict adjustment coefficient, conflict equivalent, length of conflict section and length of conflict zone, evacuation equivalent unit conflict value of conflict zone (i, j) is given as

ISSN: 1813-4890

$$x_{ij} = \sum_{s,s' \in S} \sum_{d,d' \in D} a_s \cdot \frac{Q_{sdij} \cdot Q_{s'd'ji} \cdot l_{ij}}{\sum_{(i,j) \in E} l_{ij}}, \tag{5}$$

where, $Q_{s'd'ji}$ represents the conflict equivalent from starting point s' to exit node d', and $s \neq s'$, $d \neq d'$. l_{ij} represents the length of conflict section (i, j).

4. Algorithm design

4.1. K-means clustering

This study employs K-means clustering to analyze the evacuation equivalent unit conflict values for each conflict section, thereby identifying the conflict sections with higher risk levels. Specifically, K-means clustering is a classic unsupervised learning method that assigns samples to the nearest cluster center through the Lloyd algorithm, and continuously updates the cluster center positions to achieve clustering. The algorithm aims to minimize the sum of squared distances between samples within the cluster and their corresponding cluster centers, thereby enhancing intra-cluster similarity and inter-cluster differentiation. The steps of the K-means clustering method are as follows.

Step 1: Sort the evacuation equivalent unit conflict values corresponding to each road section in ascending order from small to large. Evacuation equivalent unit conflict value is obtained as

$$X^1 = (x_1^1, x_2^1, \cdots, x_L^1). \tag{6}$$

where, X^1 represents the sorted evacuation equivalent unit conflict value vector. x_1^1 represents evacuation equivalent unit conflict value, with a cardinality of L. x_L is divided into 3 categories. Let virtual evacuation equivalent unit conflict values μ_n $(n = 1,2,3)$ are assumed as the initial clustering center, it gets $\mu_1 = x_1^1$, $\mu_2 = x_{\lfloor L/2 \rfloor}^1$, $\mu_3 = x_L^1$.

Step 2: Take any $x_m^1 \in \mathrm{M}^1$, calculate the distance of x_m^1 $(1 < m < L)$ and μ_n $(n = 1,2,3)$, and the result is $d(x_m^1, \mu_n)$. Let $\mathrm{M}(x_m^1) = \mu_n^*$, where $\mu_n^* \in \{\mu_n | n = 1,2,3\}$. It is satisfied to $d(x_m^1, \mu_n^*) = \min_{n=1,2,3} d(x_m^1, \mu_n)$. By substituting all the elements in X^1 into function $\mathrm{M}(\cdot)$ in turn, it obtains a vector

$$K_1 = (\mathrm{M}(x_1^1), \mathrm{M}(x_2^1), \cdots \mathrm{M}(x_L^1)). \tag{7}$$

In that, each evacuation equivalent unit conflict value points to the second-generation class $V_1(\mu_1), V_1(\mu_2), V_1(\mu_3)$.

Step 3: Take any $n \in \{1,2,3\}$, it gets

$$C(\mu_n) = \left\{ x_{\mu_n}^{2,v} \middle| x_{\mu_n}^{2,v} \in V_1(\mu_n); v = 1,2,\cdots, \varphi(V_1(\mu_n)); d(x_{\mu_n}^{2,v-1}, \mu_n) \leq d(x_{\mu_n}^{2,v}, \mu_n) \right\}. \tag{8}$$

It is assumed that $\mu_n^1 = x_{\mu_n}^{2,\left\lfloor \frac{\varphi(C(\mu_n))}{2} \right\rfloor}$. $\varphi(V_1(\mu_n))$ represents the cardinality of $V_1(\mu_n)$. $\varphi(C(\mu_n))$ represents the cardinality of $C(\mu_n)$. Let μ_n^1 $(n = 1,2,3)$ represents virtual clustering center in the second generation . In that, $\lfloor \cdot \rfloor$ is a function that rounds down. Calculate the distance between x_m^1 $(1 < m < L)$ and μ_n $(n = 1,2,3)$. Then, move on to Step 2 and Step 3 in sequence. Finally, the third-generation clustering center is obtained as μ_n^2.

Step 4: When there is no significant change in the cluster center or the iteration number reaches a preset threshold, the clustering iteration of each evacuation equivalent unit conflict values is

ISSN: 1813-4890

ended. The classes of evacuation equivalent unit conflict values are obtained as $V_r(\mu_n)$, $(n=1,2,3)$, where r represents iteration number.

4.2. Solution process

This study divides starting points into 8 areas based on the positions of starting points and four intersections. The pseudo-code of the algorithm is shown in Table 1. The overall solution process is as follows.

Step 1: Establish a topological graph and initialize parameters. Obtain the number of people at each starting point and the length of each road segment. Define the set of starting points, corridor nodes and exit nodes.

Step 2: Obtain path assignment probabilities. Plan paths from starting points within each area to the four exits, and calculate the length of each path. Compute the utility function for each starting point to different exits, and obtain the path assignment probabilities for each exit.

Step 3: Calculate the evacuation equivalent of the conflict zone. Obtain the conflict zones corresponding to each path through pairwise comparisons, and acquire the conflict road segments and the length of the conflict zones. Determine the evacuation equivalent of each road segment on the conflict zone based on the number of people to be evacuated, path allocation probability, and evacuation equivalent coefficient.

Step 4: Calculate the evacuation difficulty adjustment coefficient for the starting point. Obtain the distance from each starting point to the nearest exit, and based on the distance from each starting point to the exit and the total number of starting points, provide a conflict adjustment coefficient. Furthermore, revise the evacuation equivalent of each conflict zone using the conflict adjustment coefficient.

Step 5: Calculate the evacuation equivalent unit conflict value for each conflict zone and accumulate it onto each road segment. Finally, obtain the heat distribution map of the evacuation equivalent unit conflict value for each road segment on the Ro-Ro passenger ship.

Step 6: Based on K-means clustering method, the evacuation equivalent unit conflict values of each road segment are analyzed to obtain three types of clustering results.

It is noteworthy that the calculation method for the shortest path length corresponding to each of the 8 areas is related to the position of the starting point relative to the intersections. Concretely, when the path turns twice, the route from the starting point to the exit consists of three parts: the distance traveled horizontally along the current corridor, the vertical distance generated by completing the transition from the upper corridor to the lower corridor through a vertical passage at the intersection, and the horizontal distance along the target corridor to the exit after the transition. When the path turns once, the route from the starting point to the exit consists of two parts: the distance traveled vertically along the current corridor to reach the upper or lower corridor, and the horizontal distance along the target corridor to the exit after the transition. When the path does not turn, the route from the starting point to the exit is the distance traveled horizontally along the current corridor. This calculation method determines the number of turns for each path and the length of each path based on different areas. This method effectively reduces the number of candidate paths and redundant calculations, while clearly reflecting the path selection and detour methods under different exit directions, with good interpretability.

ISSN: 1813-4890

Table 1 The pseudo-code of the algorithm

The overall framework of the algorithm
1:Input:
2:A set of starting point coordinates, number of personnel at each starting point, a set of exit coordinates, a set of corridor coordinates, weight coefficient, turning coefficient, the maximum length of path, number of starting points, evacuation equivalent coefficient and number of clusters in K-means clustering
3:Output:
4: The evacuation equivalent unit conflict values and clustering results for each road segment
5: The process of the algorithm:
6: Generate routes to each exit based on different regions and calculate allocation probabilities of routes:
7: For each starting point in regions 1-8:
8: Generate paths to various exits based on different areas. If there are two path options, generate them together.
9: Sort the length values from each starting point to the four exits based on the path length:
10: The length value for each starting point:
11: The corrected length value equals the ranking multiplied by the path length.
12: Determine the value y_{sd} based on the turning conditions of each path.
13: Calculate the value of the utility function.
14: Calculate path selection probability.
15: Calculate the conflict adjustment coefficient and the evacuation equivalent corresponding to each starting point to the exit node.
16: Convert each path into a sequence of road segments that are sequentially traversed from the starting point to the end point. If there are two path options, generate two corresponding road segment sequences simultaneously.
17: Compare different road segment sequences pairwise:
18: If two road segments have the same endpoints in reverse order, they are identified as a conflict segment within a conflict zone.
19: For each pair of path sequences, the conflict-zone length is determined from the maximum and minimum x-coordinates and y-coordinates of the endpoints of the conflict segments.
20: Calculate the evacuation equivalent unit conflict value for each road segment.
21: Calculate the sum of the evacuation equivalent unit conflict values for each road segment.
22: Analyse evacuation equivalent unit conflict values of each road segment based on K-means clustering.
23: Obtain three types of clusters.

4.3. Solution process

To determine cluster number, elbow method is employed in this study. The elbow method compares the within-cluster sum of squares under different cluster numbers and selects the knee point where the decreasing trend changes from fast to slow as the optimal number of clusters. The within-cluster sum of squares is given as

$$SSE(K)=\sum_{k=1}^{n}\sum_{\mu_L\in C_k}\left\|x_L-\mu_n\right\|^2. \tag{9}$$

where, K represents the number of clusters, C_k represents the cluster k, μ_k represents the center of the cluster k.

ISSN: 1813-4890

This study employs contour coefficient, Calinski-Harabasz index, and Davies-Bouldin index to evaluate clustering results. The silhouette coefficient comprehensively measures the within-cluster compactness and between-cluster separability of samples, with a value range of [-1, 1]. A larger silhouette coefficient indicates a better clustering effect, and it is generally considered that a value above 0.5 is acceptable. The silhouette coefficient is given as

$$SC = \frac{1}{L}\sum_{l=1}^{L} s(i) = \frac{1}{L}\sum_{l=1}^{L} \frac{a(i)-b(i)}{\max\{a(i),b(i)\}}. \tag{10}$$

where, $a(i)$ represents the average distance between the sample x_L and the samples within the same cluster. $b(i)$ represents the minimum average distance between the sample x_L and the samples within the other cluster. Calinski-Harabasz index evaluates clustering quality based on the ratio of between-class dispersion to within-class dispersion. The larger the value, the clearer the clustering structure. Calinski-Harabasz index is given as

$$CH(K) = \frac{Tr(B_k)/(n-1)}{Tr(W_k)/(L-n)}. \tag{11}$$

where, $Tr(B_k)$ represents the trace of a matrix. B_k and W_k represents The between-class scatter matrix and within-class scatter matrix, which are given as

$$B_k = \sum_{k=1}^{n} |C_k| (\mu_k - \bar{\mu})(\mu_k - \bar{\mu})^T \tag{12}$$

$$W_k = \sum_{k=1}^{n} \sum_{\mu_L \in C_k} (x_L - \mu_k)(x_L - \mu_k)^T \tag{13}$$

where, $\bar{\mu}$ represents global mean. Davies-Bouldin index measures the separability between clusters by comparing the relative ratio of within-cluster dispersion to between-cluster center distance. A smaller Davies-Bouldin index indicates a better clustering effect, and it is generally considered that a value less than 0.5 is excellent. The Davies-Bouldin index is given as

$$DB(K) = \frac{1}{n}\sum_{k=1}^{n} \max_{i \neq j} \frac{C_i + C_j}{M_{ij}}. \tag{14}$$

where, $S_i = \frac{1}{|C_i|}\sum_{x \in C_i} \|x_i - \mu_i\|$ represents intra-cluster divergence, $M_{ij} = \|\mu_i - \mu_j\|$ represents inter-cluster center distance. C_i and C_j represents the clusters i and j. x_i represents the sample i. μ_i and μ_j the center of clusters i and j.

5. Results and discussion

5.1. Parameter settings

This study takes a Ro-Ro passenger ship as a practical case. The ship is divided into four MVZs. One MVZ on deck 8 as the research object is selected, which has a total of 42 rooms. Among them, 26 rooms are connected to transverse corridors, with 2 people in each room. 16 rooms are connected to longitudinal corridors, with four people in each room. The coordinates of the four exit nodes are (0, 6.4), (38, 6.4), (0, 19), and (38, 19). The coordinates of the intersections of the four transverse and longitudinal corridors are (9.5, 6.4), (19.2, 6.4), (9.5, 19), and (19.2, 19). Fig. 4 is the topological diagram of the selected MVZ.

ISSN: 1813-4890

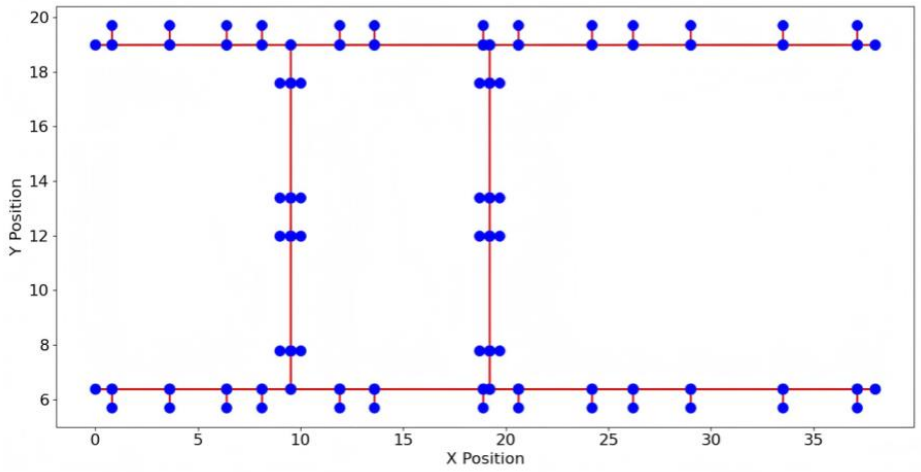

Fig. 4 Topological diagram of a MVZ on the eighth deck of a Ro-Ro passenger ship

After generating the heatmap, this study clusters each evacuation equivalent unit conflict value to obtain the risk degree of each conflicting road segment. To verify the effectiveness of the K-means clustering method, this study compares the K-means clustering method with the DBSCAN clustering method, and sets up six evacuation scenarios based on conflict adjustment coefficients, turning coefficients, and conflict equivalent coefficients. The number of clusters for K-means clustering is assumed to be 3. Meanwhile, DBSCAN clustering method is a density-based clustering method, and the value settings of its neighborhood radius *eps* and the minimum number of points *mineps* depend on the characteristics of the dataset and directly affect the quality of the clustering results. The coordinates of each starting point are shown in Table 2. The different evacuation scenarios and their corresponding parameters of DBSCAN clustering method are shown in Table 3.

Table 2 The coordinates of starting points

Serial number	Coordinate	Serial number	Coordinate	Serial number	Coordinate
1	(0.8,5.7)	2	(3.6,5.7)	3	(6.4,5.7)
4	(8.1,5.7)	5	(11.9,5.7)	6	(13.6,5.7)
7	(18.9,5.7)	8	(20.6,5.7)	9	(24.2,5.7)
10	(26.2,5.7)	11	(29,5.7)	12	(33.5,5.7)
13	(37.1,5.7)	14	(0.8,19.7)	15	(3.6,19.7)
16	(6.4,19.7)	17	(8.1,19.7)	18	(11.9,19.7)
19	(13.6,19.7)	20	(18.9,19.7)	21	(20.6,19.7)
22	(24.2,19.7)	23	(26.2,19.7)	24	(29,19.7)
25	(33.5,19.7)	26	(37.1,19.7)	27	(9,7.8)
28	(9,12)	29	(9,13.4)	30	(9,17.6)
31	(10,7.8)	32	(10,12)	33	(10,13.4)
34	(10,17.6)	35	(18.7,7.8)	36	(18.7,12)
37	(18.7,13.4)	38	(18.7,17.6)	39	(19.7,7.8)
40	(19.7,12)	41	(19.7,13.4)	42	(19.7,17.6)

Table 3 Parameter settings for different evacuation scenarios and DBSCAN

Experimental condition	Serial number	β	γ	eps	mineps
With a_s	1	0.5	10	75000	2
	2	0	10	75000	2
	3	0.5	20	300000	2

ISSN: 1813-4890

Without a_s	4	0.5	10	25000	2
	5	0	10	25000	2
	6	0.5	20	25000	2

5.2. Comparative analysis of different evacuation scenarios

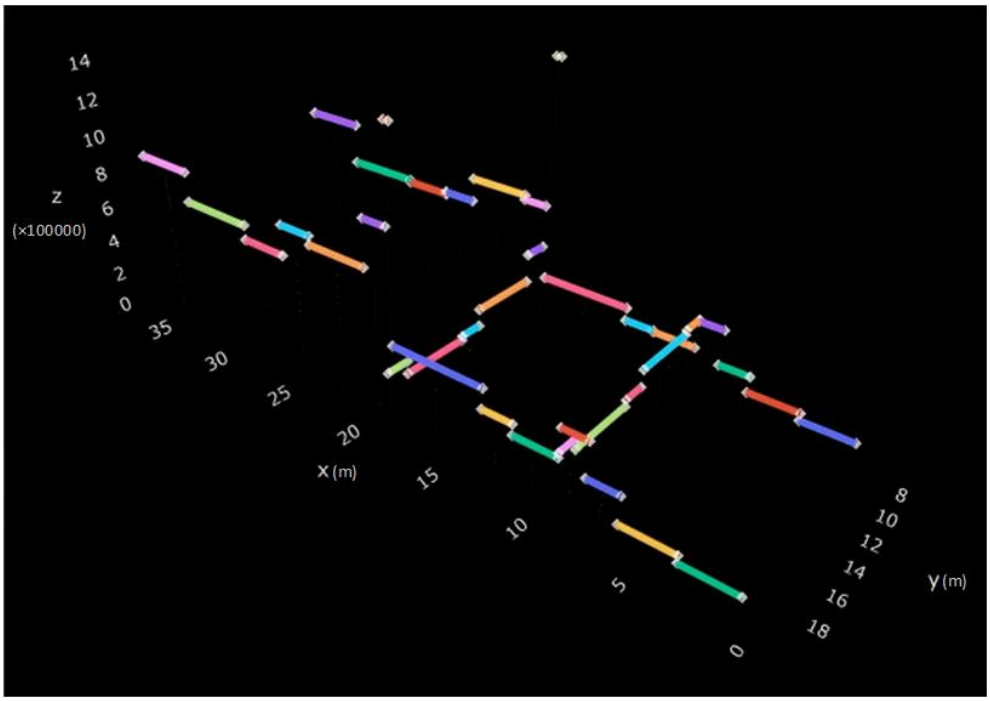

Fig. 5 Conflict value results of evacuation equivalent units in scenario 1

Table 4 Statistics of calculation results under different scenarios

Serial number	The maximum value	The minimum value	Average value	Variance	The road segment with the minimum value
1	960393.92	6540.5	290587.47	5.29×1010	((18.9, 6.4), (19.2, 6.4))
2	621840.49	3807.46	179512.83	1.94×1010	((18.9, 6.4), (19.2, 6.4))
3	2487361.94	15229.83	718051.31	3.11×1011	((18.9, 6.4), (19.2, 6.4))
4	264417.52	1787.28	76634.02	3.76×109	((18.9, 6.4), (19.2, 6.4))
5	169563.07	1061.75	47132.56	1.38×109	((18.9, 6.4), (19.2, 6.4))
6	678252.28	4247.02	188530.23	2.21×1010	((18.9, 6.4), (19.2, 6.4))

ISSN: 1813-4890

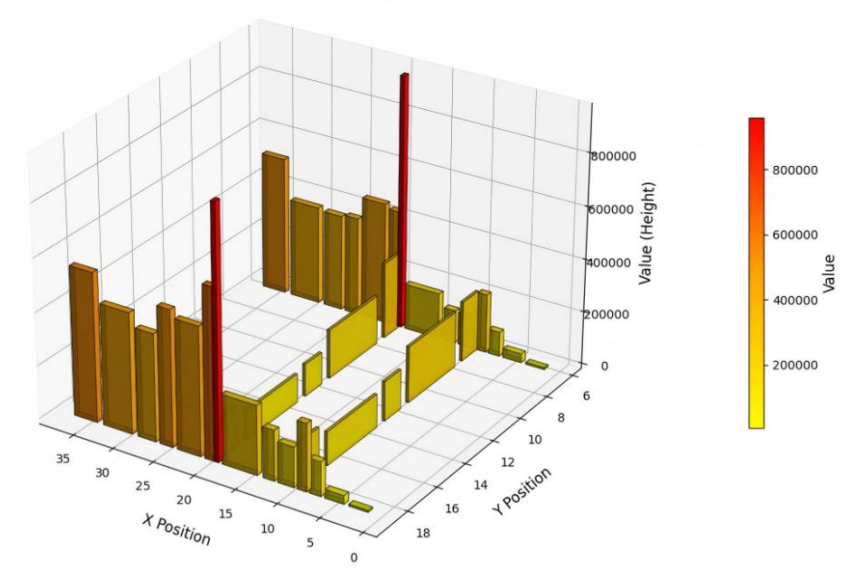

Fig. 6 Heat map of evacuation equivalent unit conflict value in scenario 1

Fig. 5 presents the evacuation equivalent unit conflict values under Scenario 1. As shown in Fig. 5, the evacuation equivalent unit conflict values for the sections directly connected to the four exits are 0. Thus, the evacuation situation of these sections will not be analyzed in this paper. There are significant differences in evacuation equivalent unit conflict values among the remaining 38 sections. The maximum evacuation equivalent unit conflict value is 960,393.92, while the minimum is 6,540.5. The section with the highest evacuation equivalent unit conflict value is the intersection of the horizontal and vertical corridors, which is located far from the MVZ exit. The results indicate that this method effectively identifies main risk areas during evacuation.

Fig. 6 provides a heat map of the evacuation equivalent unit conflict value under scenario 1, reflecting the spatial distribution of the risk of personnel falling. As shown in Fig. 6, the longitudinal coordinates of nodes in the longitudinal corridor along the ship's bow-to-stern line indicate that a translation perpendicular to the ship's bow-to-stern line towards the bow or stern will result in changes in the conflict equivalent near the exit of the main vertical zone. When there are two longitudinal corridors, the conflict equivalent is lower in the transverse corridor near the exit of the MVZ, and higher in the transverse corridor farther from the exit of the main vertical zone. This indicates that being far away from the evacuation exit is the main factor leading to an increase in the evacuation equivalent unit conflict value. This method provides a clear decision-making basis for the optimization of evacuation facility layout.

To compare the calculation results under different scenarios, Table 4 presents the statistics of the evacuation equivalent unit conflict values under six scenarios. As shown in Table 4, there are significant differences in the statistical results when the conflict adjustment coefficient, turning coefficient, and conflict equivalent coefficient take different values. It is noteworthy that the maximum evacuation equivalent unit conflict values in all six scenarios occur at the intersections of horizontal and vertical corridors that are farther away from the main vertical zone exit. It indicates that under different coefficients, the probability of falls in this area remains the highest, making it a main area for evacuation facility layout. This phenomenon is due to the significant increase in the probability and number of people passing through the intersection, which leads to an increase in the evacuation equivalent unit conflict values. Additionally, this study determines the distance ratio based on the front and rear positions of each passage section in the longitudinal profile of the ship's MVZ. Table 4 illustrates significant differences in the variance under different conflict adjustment coefficients. It indicates that after employing a conflict adjustment coefficient, evacuation equivalent unit conflict values

ISSN: 1813-4890

increase, and the fluctuations of different passage sections also show an increasing trend. The results in Table 4 verify the effectiveness of this calculation method, reflect its ability to identify key risk areas, and illustrate its applicability in the evacuation process of MVZ.

5.3. Comparative analysis of different clustering methods

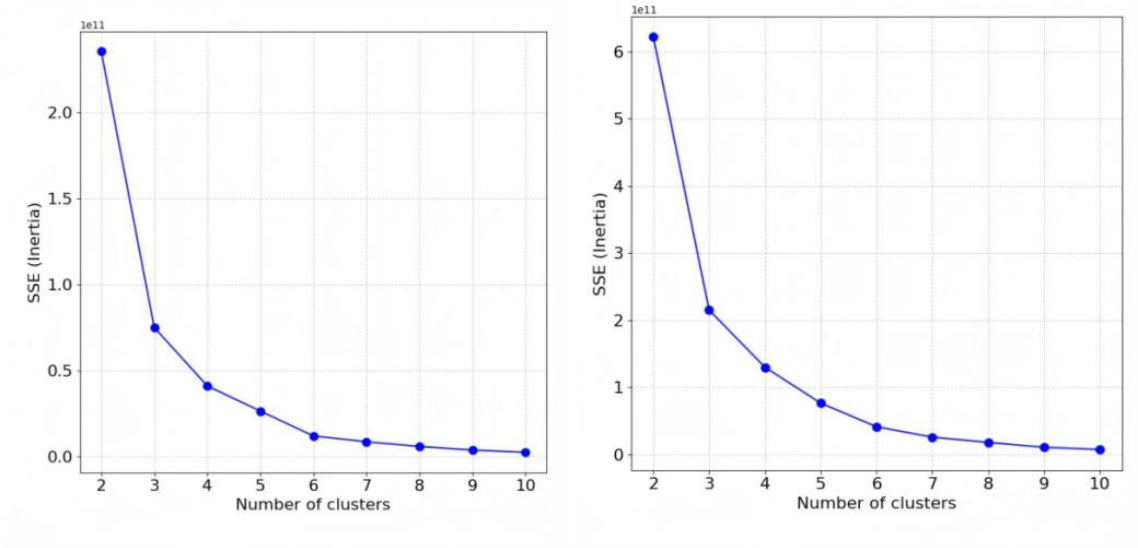

(a) Scenario 1

(b) Scenario 2

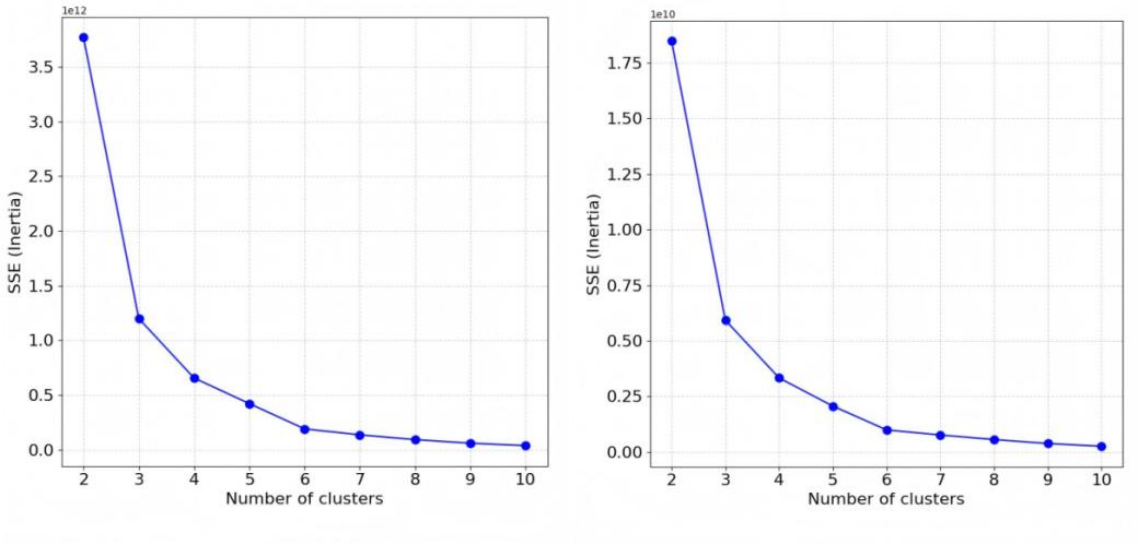

(c) Scenario 3

(d) Scenario 4

ISSN: 1813-4890

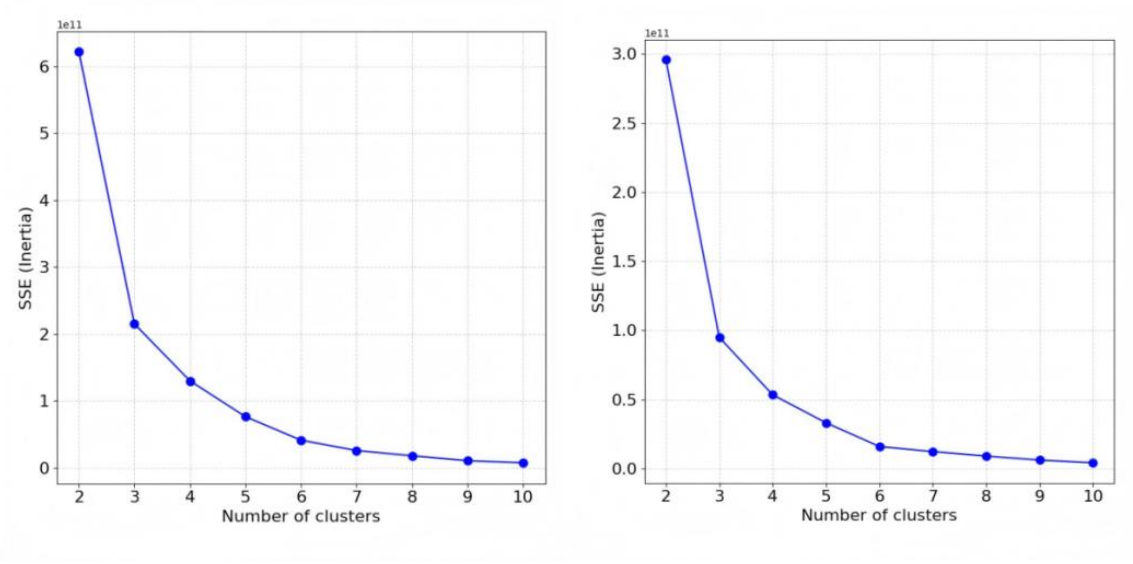

(e) Scenario 5 (f) Scenario 6

Fig. 7 Determining the number of clusters for K-means clustering by the elbow method

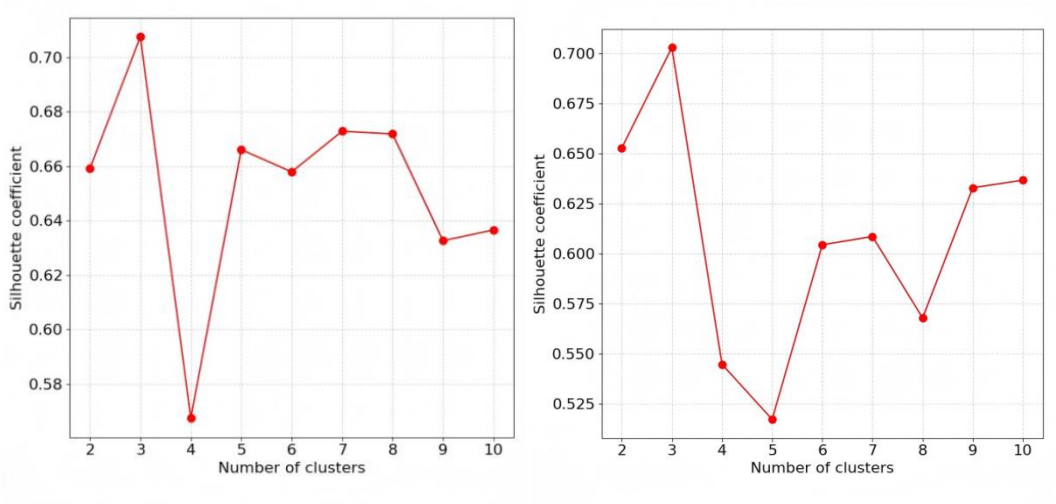

(a) Scenario 1 (b) Scenario 2

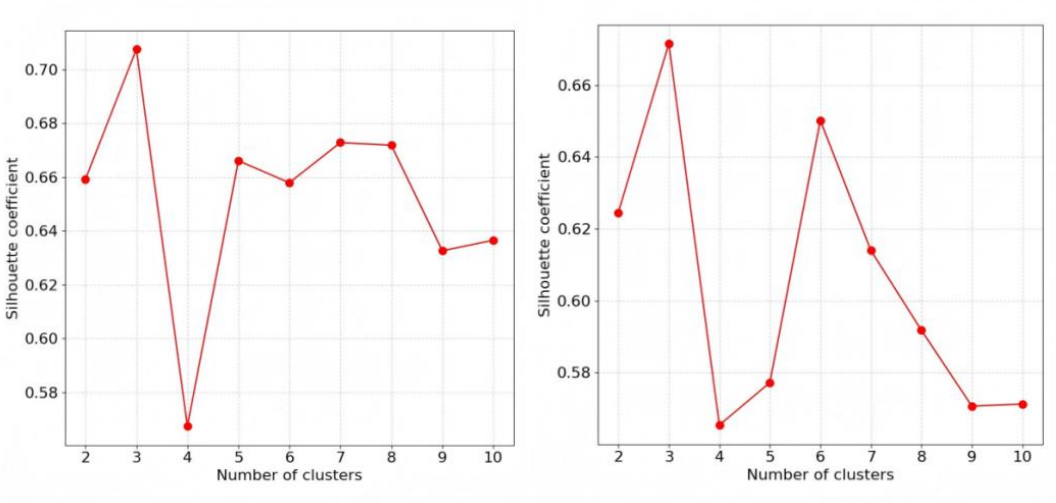

(c) Scenario 3 (d) Scenario 4

ISSN: 1813-4890

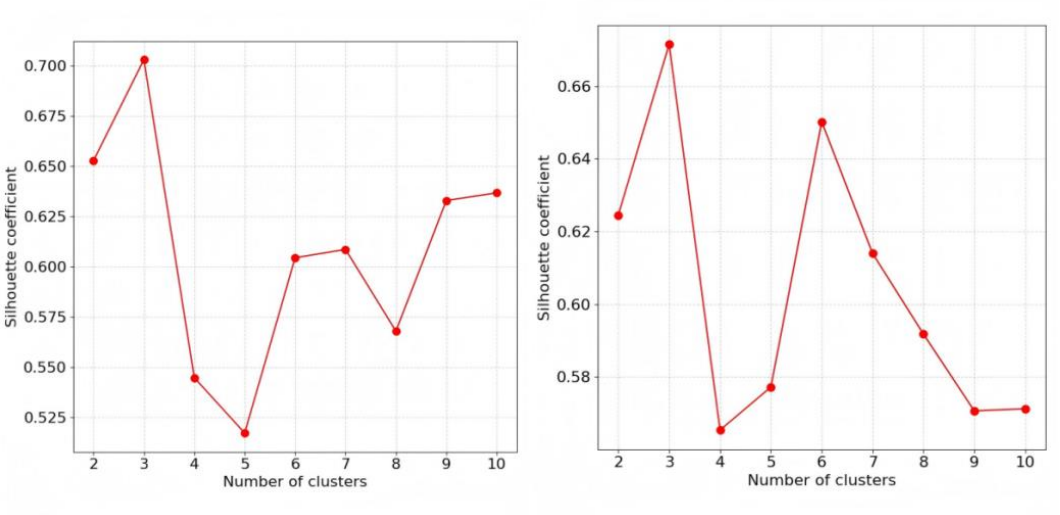

(e) Scenario 5 (f) Scenario 6

Fig. 8 K-means clustering contour coefficient under different cluster numbers

To verify the effectiveness of the selected cluster number, Fig. 7 presents the elbow method to validate the results of K-means clustering method. As shown in Fig. 7, the within-cluster distance decreases as the number of clusters increases; however, when the number of clusters exceeds 3, the rate of decrease slows significantly. In this scope, the decrease in within-cluster distance slows down significantly. This inflection point is set as the elbow, representing a critical turning point for improving clustering performance. Specifically, when the number of clusters is 3, the within-cluster distance converges significantly, which ensures clustering performance and limits computational complexity. If the number of clusters continues to increase, it results in similar clustering performance but a significant increase in computational complexity.

To verify the effectiveness of K-means clustering, Fig. 8 illustrates the silhouette coefficients of K-means clustering under different cluster numbers. For cluster numbers ranging from 2 to 10, the clustering results and silhouette coefficients are calculated. As shown in Fig. 8, when the cluster number is 3, the silhouette coefficients for all six scenarios reach their maximum values, all of which are higher than evaluation criteria of 0.5. When the cluster number is greater than 3, silhouette coefficients decrease as the cluster number increases significantly. Therefore, selecting a cluster number of 3 is deemed the optimal configuration. In conclusion, the results in Fig. 7 and Fig. 8 verify the rationality and feasibility of this cluster number selection.

To determine the risk degree of each road segment, Table 5 provides the results of K-means clustering method under 6 scenarios. As shown in Table 5, calculation results of K-means clustering method indicate that the road segments in the MVZ on Deck 8 are clustered into three categories, which involve high, medium, and low. From Fig. 6 and Table 4, it is seen that in scenario 4, the intersection located farther from the exit of the MVZ has the highest evacuation equivalent unit conflict value for the two corresponding road segments, belonging to the first category. The road segments near the exit of the main vertical area in the longitudinal corridor and the 12 adjacent road segments belong to the second category, while the others belong to the third category. Similar clustering results were obtained in other scenarios. Table 5 verifies the feasibility of the K-means clustering method.

To verify the performance of the K-means clustering, Table 6 presents the clustering results obtained by using the DBSCAN clustering method under different evacuation scenarios, and the clustering results are validated by silhouette coefficient, Calinski-Harabasz index, and Davies-Bouldin index. DBSCAN clustering meets the evaluation criteria in scenarios 1, 3, 4, 5, and 6, but only forms two clusters. Specifically, in scenario 2, the method forms three clusters, but with one outlier. It also indicates that the results of DBSCAN clustering fluctuate with changes in

evacuation scenarios, lacking consistency. In contrast, the results of K-means clustering form similar three clusters in six scenarios, demonstrating strong stability and a certain degree of interpretability. The comparative experiment between the two methods shows that K-means clustering method performs better in classifying evacuation equivalent unit conflict values compared to the DBSCAN clustering algorithm.

Table 5 The results of K-means clustering

Serial number	Cluster	Central value	Number of points
1	High	953753.33	2
	Medium	466442.12	12
	Low	147396.32	24
2	High	589549.55	2
	Medium	283354.41	12
	Low	93422.31	24
3	High	2358198.20	2
	Medium	1133417.63	12
	Low	373689.24	24
4	High	259926.63	2
	Medium	117956.86	13
	Low	37339.15	23
5	High	158826.54	2
	Medium	73231.66	12
	Low	24775.17	24
6	High	635306.17	2
	Medium	292926.64	12
	Low	99100.69	24

Table 6 Evaluation index results of DBSCAN clustering under different evacuation scenarios

Serial number	The number of clusters	The number of noise points	Silhouette coefficient	Calinski-Harabasz index	Davies-Bouldin index
1	2	0	0.7062	35.15	0.2709
2	3	1	0.7111	154.42	0.2880
3	2	0	0.7062	35.15	0.2709
4	2	0	0.7178	38.37	0.2772
5	2	0	0.7202	37.54	0.2155
6	2	0	0.7178	38.37	0.2772

6. Conclusion

This study proposes an evacuation layout optimization method based on probability assignment and K-means clustering to address the evacuation problem within an MVZ of Ro-Ro passenger ships. The impact of conflict equivalence on evacuation layout is analysed, which provides decision support for the layout of evacuation facilities and surveillance cameras. The main conclusions of this study are as follows.

Firstly, this study determines the distance ratio of each passage segment based on the position of MVZ in the longitudinal profile of the ship.

Secondly, in the direction of the ship's bow-to-stern line, the longitudinal coordinates of nodes perpendicular to the ship's bow-to-stern line will change the probability of falling near the exit of the main vertical zone when translating towards the bow or stern. When there are two longitudinal corridors, the intersection between the longitudinal corridor closer to the main

vertical zone exit and the adjacent section has a lower probability of falling; the intersection between the longitudinal corridor farther from the main vertical zone exit and the adjacent section has a higher probability of falling.

Thirdly, the highest point of conflict equivalence occurs at the intersection of the horizontal corridor and the vertical corridor, which is relatively far from the exit of MVZ.

Fourthly, the calculation results of the evacuation equivalent unit conflict value indicate that the road sections in MVZ on deck 8 under study are clustered into three categories. Among them, the intersections located farther from the exit of MVZ have the highest evacuation equivalent unit conflict values for the two corresponding road sections, belonging to the first category. The longitudinal corridor between the intersection farther from the main vertical zone exit and the main vertical zone exit belongs to the second category, while the others belong to the third category.

However, this study still has certain limitations. In the future, the applicability of the proposed method to other types of passenger vessels, such as cruise ships, will be verified.

References

[1] Z.C. He, K.S. Shen, M. Lan, et al.: An evacuation path planning method for multi-hazard accidents in chemical industries based on risk perception. Reliability Engineering and System Safety, vol. 244 (2023), p.109912.

[2] X.X. Yang , W.K. Dai, Y.X. Li, et al.: An efficient evacuation path optimization for passengers in subway stations under floods. Tunnelling And Underground Space Technology, vol. 143(2024), p.105473.

[3] Y.Q. Zhang, J.H. Wang, Y. Wang, et al.: Intelligent planning of fire evacuation routes in buildings based on improved adaptive ant colony algorithm. Computers & Industrial Engineering, vol. 194 (2024), p.110335.

[4] C.J. Rodrigues, L. Tralhão, L. Alçada-Almeida: Solving a location-routing problem with a multiobjective approach: the design of urban evacuation plans. Journal of Transport Geography, vol. 22 (2012), 206-218.

[5] Y. Gu, H.Q. Tan, A. Chen, et al.: A multiplicative regret-based stochastic user equilibrium model. Transportation Research Part B: Methodological, vol. 204 (2026), p.103362.

[6] T.K. Rasmussen, L.C. Duncan, D.P. Watling, et al.: Local detouredness: A new phenomenon for modelling route choice and traffic assignment. Transportation Research Part B: Methodological, vol. 190 (2024), p.103052.

[7] G.Y. Qin, S.D. Deng, Q. Luo, et al.: Multimodal traffic assignment from privacy-protected OD data. Communications in Transportation Research, vol. 5 (2025), p.100223.

[8] Z. Islam, M. Abdel-Aty: Traffic conflict prediction using connected vehicle data. Analytic Methods In Accident Research, vol. 39 (2023), p.100275.

[9] N. Park, J. Park, Y.J. Joo, et al.: Micro-level hotspot identification at intersections using traffic conflict analysis. Accident Analysis & Prevention, vol. 220 (2025), p.108167.

[10] A. Arun, M.M. Haque, S. Washington, et al.: How many are enough?: Investigating the effectiveness of multiple conflict indicators for crash frequency-by-severity estimation by automated traffic conflict analysis. Transportation Research Part C: Emerging Technologies, vol. 138 (2022), p.103653.

[11] I.M. Islam, A. Alogaili: Uncovering the risks for driver injury severities for truck-trailer and passenger car crashes at highway-railroad crossings. Transportation Research Interdisciplinary Perspectives, vol. 31 (2025), p.101451.

[12] Michael D J: Beyond Chinese Ferry Tales: The Rise of Deck Cargo Ships in China's Military Activities, 2023 (China Maritime Studies Institute, American 2024)